Zirconia and Zirconia−ORMOSIL Planar Waveguides Prepared at Room Temperature

Y. Sorek, M. Zevin, and R. Reisfeld*,†

Inorganic and Analytical Chemistry Department, The Hebrew University of Jerusalem, Givat-Ram, 91904 Jerusalem, Israel

T. Hurvits and S. Ruschin

Department of Electrical Engineering—Physical Electronics, Tel-Aviv University, Tel-Aviv, Israel

Received February 15, 1996. Revised Manuscript Received December 12, 1996⊗

We describe the preparation of zirconia and hybrid zirconia−ORMOSIL planar waveguides by sol−gel technology at room temperature. Acetic acid was used as chelating agent to stabilize the zirconia precursor. Multimode light guiding was demonstrated for the first time in zirconia films prepared by the sol−gel method. The properties of the films, refraction index, thickness, and transparency as well as structural characterization using Fourier transform infrared spectroscopy, X-ray photoelectron spectroscopy (XPS), thermal analysis, and X-ray diffraction (XRD), were studied. The zirconia film contains propoxy, acetate, and hydroxyl ligands. In the zirconia−ORMOSIL films Zr−O−Si bonds were found, although homocondensation bonds are favored. The mechanism proposed for the structural results involves condensation of oligomeric species that react by ligand exchange. XRD show wide peaks at angles in area of $2\Theta = 4-10°$. These peaks can be attributed to oligomeric structures with *d* spacing values of about 10 Å. The hybrid films are hydrophobic and XPS measurements shows that the surface is covered mainly by organic groups of the ORMOSIL. Films doped by pH indicator Methyl Red showed reversible response to acid and base vapors; this opens the possibility to use such films as waveguide-based optical sensors.

Introduction

In earlier publications we reported on the preparation[1] and characterization[2] of titania−ORMOSIL waveguides prepared by the sol−gel method. The preparation procedure at low temperature allows the incorporation of organic additives that such as laser dyes[3] or indicators into the waveguide. A promising technological application of such waveguides is their use in optical sensors.[4−6] The following properties of zirconia-based films make them suitable candidates for use as waveguide sensors: (1) The high refractive index of the films enables their use as waveguides deposited on ordinary glass substrate. (2) In order to use the waveguides for environmental, biological, or industrial sensing purposes, special consideration must be given to the matrix stability to chemical damage in solution. Zirconia-containing glasses are long known to be alkali-resistant.[7] (3) Unlike titania, ZrO_2 causes no catalytic photodegradation of organic dopant. The energy gap between valence and conduction bands is much higher so the photocatalytic stage

$$M^* \rightarrow M^+ + e^-(CB) \quad (1)$$

where M* is a photoexcited molecule and e^-(CB) is the electron in the conduction band of the semiconductor, is less favorable.

It is, therefore, the aim of this work to prepare high optical quality waveguiding films based on zirconia or zirconia−polymer composites at a temperature that allows the incorporation of organic analytical reagents.

A major obstacle in preparing ZrO_2 coating from zirconium alkoxides is rapid hydrolysis and subsequent precipitation of colloidal zirconia upon water addition to $Zr(OR)_4$-containing precorsor solutions. Such fast precipitation creates difficulties in the sol−gel preparation of zirconia-based transparent glasses or coatings.

Transparent ZrO_2 coatings from solution were first prepared by Ganguli and Kundu.[8] They overcome the fast precipitation problem by dissolving zirconium propoxide in dried solvents such as 2-propanol, cyclohexane, and benzene. The hydrolysis was performed by exposure of the coatings prepared from the solution to atmospheric moisture. Baking to 450 °C was necessary to obtain transparent films. It is possible, however, to stabilize the precursor by complexing agents like acetic acid,[9,10] valeric acid,[11] or diketones exhibiting keto−enol

* To whom correspondence should be addressed.
† A member of the Farkas Center for Light Induced Processes. Enrique Berman Professor of Solar Energy.
⊗ Abstract published in *Advance ACS Abstracts,* February 1, 1997.

(1) Sorek, Y.; Reisfeld, R.; Finkelstein, I.; Ruschin, S. *Appl. Phys. Lett.* **1993**, *63*, 3256.
(2) Sorek, Y.; Reisfeld, R.; Tenne, R. *Chem. Phys. Lett.* **1994**, *227*, 242.
(3) Reisfeld, R. *J. Phys. IV* **1994**, *4*, C4−281.
(4) Lee, J. E.; Saavedra, S. S. *Anal. Chim. Acta* **1994**, *285*, 265.
(5) Chernyak, V.; Reisfeld, R.; Gvishi, R.; Venezky, D. *Sensors Mater.* **1990**, *2*, 117.
(6) Chernyak, V.; Reisfeld, R. *Sensors Mater.* **1993**, *4*, 195.
(7) Nakishima, A.; Oohashi, H.; Wakakuwa, M.; Kotani, K.; Shimohira, T. *J. Non-Cryst. Solids* **1980**, *42*, 545.
(8) Ganguli, D.; Kundu, D. *J. Mater. Sci. Lett.* **1984**, *3*, 503.
(9) Kundu, D.; Kumar Biswas, P.; Ganguli, D. *Thin Solid Films* **1988**, *163*, 273.
(10) Noonan, G. O.; Ledford, J. S. *Chem. Mater.* **1995**, *7*, 1117.
(11) Severin, K. G.; Ledford, J. S.; Torgerson, B. E.; Berglund, K. A. *Chem. Mater.* **1994**, *6*, 890.

S0897-4756(96)00135-4 CCC: $14.00

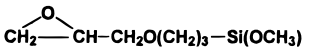

Figure 1. GLYMO: γ-glycidyloxipropyltrimethoxysilane.

tautomerization[12] such as acetylacetonate and acetoacetate. Si−O−M bonds (M = Ti, Al, or Zr) are formed by a condensation reaction between silanol groups and the ligand,[13] and the complexing additives remain in the final product as was demonstrated by IR spectroscopy and XPS. Introducing organically-modified silicates (ORMOSILs) into the films allows the control of porosity,[14] refractive index, and thickness of the coating and to improve the mechanical properties and transparency of the film without heat treatment. When organic groups are incorporated in the glass, the shrinkage is low, because the bulky organic components fills the pores between the inorganic oxide chains. The material reaches its final density at low temperature, especially if the organic groups can be cross-linked by epoxy or methacryl polymerization, as is the case for the ORMOSIL used in our research GLYMO (γ-glycidyloxipropyltrimethoxysilane). $Zr(OR)_4$ acts as a catalyst for the organic polymerization besides being a precursor for the inorganic oxide formation.[15] Hybrid zirconia−ORMOSIL glass was prepared by Nass et al.[16] from zirconium propoxide and methacryloxypropylsilane, and chelating bonding of the Zr ion to the carboxy group of the ORMOSIL was demonstrated. The Zr content in the hybrid glass obtained was only 17 mol % and the refractive index was, therefore, low (1.51).

In this work we describe the preparation procedure and the characterization of waveguiding films composed either from zirconia or from hybrid zirconia−ORMOSIL glass. Films and intermediate products of synthesis were characterized using UV−vis spectroscopy, Fourier transform infrared spectroscopy (FTIR), X-ray photoelectron spectroscopy (XPS), thermal analysis (DTA/TG and DSC), and X-ray diffraction (XRD).

Experimental Section

Materials. Zirconium *n*-propoxide (70% solution in 1-propanol, Fluka) was used as received without further purification. Glacial acetic acid (analytical grade, Frutarom, Israel), 1-propanol (analytical grade, Riedel-de-Haen), γ-glycidoxypropyltrimetoxysilane (GLYMO) (Figure 1) (analytical grade, Aldrich), Methyl Red (B.D.H.), and triply distilled water were used for solutions preparation. Soda-lime glass microscopic slides (76 × 25 × 1.5 mm, $n_D = 1.51$) were used as substrate for films deposition. Slides were received precleaned and no further cleaning was performed.

CAS Registry Numbers and Chemical Hazards. $Zr(OPr^n)_4$·PrOH [23519-77-9], highly flammable, moisture sensitive, GLYMO [2530-83-8], moisture sensitive, irritant; 1-propanol [71-23-8], flammable liquid, irritant; acetic acid [758-12-3], corrosive, hygroscopic liquid; Methyl Red [493-52-7]. Wear protective clothing, glasses and gloves in order to protect skin and eyes.

Samples Preparation. *Zirconia and Zirconia-ORMOSIL Films.* 10 mL of zirconium *n*-propoxide was mixed in hermetically closed plastic vials with 3 mL of glacial acetic acid. After half-hour of stirring, 10 mL of propanol was added. The water needed for the hydrolysis was dissolved in acetic acid (1:3 vol.). 5 mL of this solution were added slowly to the stirred mixture. To prepare Zr-GLYMO films the GLYMO was added with propanol. Coatings were made by dip coating; withdrawal speed of the substrate was 20 cm/min.

To perform preliminary checking of the sensing abilities of films and find additional information about film structure, the well-studied pH-sensitive indicator dye Methyl Red (MR) was added to zirconia and zirconia−GLYMO films. Dye was added after hydrolysis stage, when, as we assumed, no water remains. This was done in order to compare results with those of MR in titania−GLYMO films.[2]

Samples for thermal analysis were dried in the Petri dishes placed in drying oven at 40 °C for 3 days.

Samples for X-ray diffraction were heated in air at 40, 100, 250, 400, and 600 °C for 12 h.

UV−Vis Spectroscopy. Absorption spectra and interference patterns were measured on a Milton-Roy SPECTRONIC M-3000 diode array spectrophotometer.

For optical characterization we used a He−Ne laser beam coupled into the film by means of a rutile prism. The propagation constants of guided modes were determined by measuring the coupling angles into the prism. Up to seven guided modes were found. The refractive index of the film and its thickness were determined by fitting the propagation constants to a step index slab model. The term *nd* (*n* the refractive index and *d* the film thickness) was independently determined for each film from the interference pattern using the formula

$$nd(1/\lambda_1 - 1/\lambda_2) = 1 \qquad (2)$$

where λ_1 and λ_2 are wavelengths of neighboring maxima or minima.

Film Density. The film's weight was measured by weighing the substrate before film deposition and after film drying. The volume was calculated using the thickness derived from eq 2.

Element analysis was performed on Perkin Elmer 240C CHN Analyzer by combustion of the sample.

X-ray photoelectron spectroscopy (XPS) measurements were taken from the films using a KRATOS AXIS-HS setup. A nonmonochromic Mg Kα (1253.6 eV) X-ray source was used. Ar^+ ion (4 KeV, 15 mA emission current) etching of a few nanometers was performed before the measurement. The etching speed of 10 Å/min was determined using Ta_2O_5/Ta sample for calibration. The energy scale was calibrated by the C(1s) line at 284.6 eV. All data processing was done with instruments internal software (on the Sun SparcStation).

Fourier Transform Infrared Spectroscopy (FTIR). FTIR spectra were taken with a BRUKER 113V interferometer. Samples were prepared using powders in KBr discs.

X-ray Diffraction (XRD). XRD patterns were measured on Philips automatic powder diffractometer PW1710 using a Cu Kα source.

Thermal Analysis. DTA/TG (differential thermal analysis/thermogravimetry) measurements were done on the TA Instruments 2100 thermal analyzer. The samples were placed in platinum crucibles and heated in air with the heating rate of 10 °C/min (Al_2O_3 as reference).

DSC (differential scanning calorimetry) measurements were performed on the TA Instruments DSC2010 differential scanning calorimeter. The samples were placed in hermetically closed aluminum capsules and heated in argon atmosphere with heating rate of 10 °C/min.

Tables. The refractive indices measured and calculated from Clausius−Mossoti equation, thickness, and density of the films are presented in Table 1. The data of XPS measurements presented in Table 2.

(12) Pashev, P.; Slavova, V. *Mater. Res. Bull.* **1992**, *27*, 1269.
(13) Abe, Y.; Sugimoto, N.; Nagao, Y.; Misano, T. *J. Non-Cryst. Solids* **1989**, *108*, 150.
(14) Sorek, Y.; Reisfeld, R.; Weiss, A. M. *Chem. Phys. Lett.* **1995**, *244*, 371.
(15) Philipp, G.; Schmidt, H. *J. Non-Cryst. Solids* **1986**, *82*, 31.
(16) Nass, R.; Schmidt, H.; Arpac, E. In *Sol-Gel Optics*; Mackenzie, J. D., Ulrich, D. R., Eds.; SPIE Proc. SPIE: Bellingham, WA, **1990**; Vol. 1328, p 258.

Table 1. Compositions and Properties of Zirconia and Zirconia−GLYMO Films

film	ZrO_2 (mol %)	n measured	n expected[a]	thickness (μm)	density (measd) (g/cm^3)
A	100	1.79	2.15	0.86	4.1
B	55	1.69	1.78	2.1	2.6
C	43	1.62	1.69	2.75	2.6
D	31	1.57	1.61	2.44	2.5

[a] Calculated using Clausius−Mossoti equation: $(n^2 - 1)/(n^2 + 2) = (4\pi/3)[V_1\alpha_1 + V_2\alpha_2]$, where V_1, α_1, V_2, and α_2 are vol % and polarizabilities of each component.

Table 2. XPS Data of Zirconia and Zirconia−ORMOSIL Films

peak	binding energy (eV)	fwhm (eV)	atomic conc (%)	mass conc (%)
		Film A		
Zr 3d (1)	182.2	0.97	7.63	29.29
Zr 3d (2)	182.9	1.05	4.82	18.51
O 1s (1)	529.8	1.28	11.35	7.64
O 1s (2)	531.5	1.5	36.08	24.29
C 1s (1)	284.1	0.9	23.42	11.83
C 1s (2)	286.2	1.13	3.70	1.87
C 1s (3)	288.8	1.31	13.00	6.56
		Film B[a]		
Zr 3d	182.3	1.46 (1.43)	4.78 (14.46)	23.73 (48.65)
Si 2p	101.9	1.66 (1.85)	6.24 (12.95)	9.54 (13.42)
O 1s	531.7	2.19 (0.67)	39.76 (39.24)	34.61 (23.16)
C 1s (1)	284.6	1.62 (1.78)	21.56 (24.57)	14.08 (10.88)
C 1s (2)	286.0	1.54 (1.77)	24.15 (5.10)	15.77 (2.26)
C 1s (3)	288.6	1.51 (3.24)	3.50 (3.68)	2.29 (1.63)
		Film C[a]		
Zr 3d	182.3	1.30 (1.50)	3.55 (7.92)	18.76 (33.00)
Si 2p	102.1	1.43 (1.94)	5.78 (13.09)	9.42 (16.81)
O 1s (1)	530.2	1.52 (1.44)	5.10 (6.86)	4.73 (5.02)
O 1s (2)	531.9	1.93 (2.21)	32.68 (30.65)	30.30 (22.41)
C 1s (1)	284.6	1.53 (1.66)	20.20 (29.83)	14.05 (16.36)
C 1s (2)	286.1	1.50 (1.85)	30.00 (9.98)	20.87 (5.47)
C 1s (3)	288.5	1.66 (1.77)	2.69 (1.68)	1.87 (0.92)
		Film D		
Zr 3d	182.4	1.44	2.32	12.82
Si 2p	101.8	1.37	7.5	12.80
O 1s (1)	529.9	1.52	3.86	3.75
O 1s (2)	532.0	1.82	31.96	31.03
C 1s (1)	284.6	1.43	19.16	13.95
C 1s (2)	286.0	1.47	33.24	24.21
C 1s (3)	288.6	1.48	1.96	1.43

[a] In the parenthesis: data after sputtering. It should be taken as approximate only.

Results

Synthesis. During preparation a white colloidal precipitate appeared either during water dropping to the solution or before the addition of the propanol and water. The chemical analysis of this primary precipitate yielded 19.15 wt % carbon and 2.93 wt % hydrogen (in addition to zirconium and oxygen). The carbon and hydrogen contents are lower than expected for stoichiometry of any combination of $Zr(OPr^n)_{4-x}(OAc)_x$ (Pr^n = n-C_3H_7, Ac = CH_3CO).

The precipitate was pepticized by adding more water to the solution. After the disappearance of the precipitate the solution is extremely stable, and no turbidity is developed even at long period (up to two months) of storage in a closed container. These observations can be explained by the following mechanism:

1. Upon adding acetic acid a ligand exchange reaction occurs to form zirconium propoxide acetate according to (3):

$$Zr(OPr^n)_4 + x\text{Ac-OH} \rightarrow Zr(OPr^n)_{4-x}(OAc)_x + x\text{Pr-OH} \quad (3)$$

2. At this stage when both zirconium acetate and propoxide are present in the solution a nonhydrolytic oxide formation is possible[17] according to (4):

$$2Zr(OPr)_{4-x}(OAc)_x \rightarrow Zr_2O(OAc)_{2x-1}(OPr)_{8-2x-1} + \text{AcOPr} \quad (4)$$

The above reaction can explain the low organic content of the precipitate caused by replacing organic groups by oxo-groups.

3. Adding water to the solution promotes hydrolysis of zirconium propoxyacetate oligomers. At this stage stable soluble species of oligomeric zirconium oxide−alkoxy acetate are formed.

The hydrolysis of zirconium propoxyacetate can be started before addition of water and can be promoted by "internal" water, produced in an esterification reaction between acetic acid and propanol[18] (It should be noted, that we use 70% solution of $Zr(OPr^n)_4$ in propanol):

$$Zr(OPr)_{4-x}(OAc)_x + yH_2O \rightarrow Zr(OAc)_x(OPr)_{4-x-y}(OH)_y + y\text{PrOH} \quad (5)$$

There can occur also condensation reaction, leading to formation of products similar of those of reaction 4:

$$2Zr(OPr)_{4-x-y}(OAc)_x(OH)_y \leftrightarrow Zr_2(OAc)_{2x}(OPr)_{8-2x-y}(OH)_y + H_2O \quad (6)$$

To determine which of the two reaction mechanisms, (4) or (5) and (6), is preferred, detailed FTIR analysis of the residual liquid has been prepared and the results will be published in our next paper.

Optical Characterization. The refractive indices of the films (Table 1) are higher than the values reported by Wang and Wilkes[19] for ZrO_2−PMTO (triethoxysilane-capped poly(tetramethylene oxide)) hybrid where $\lim_{x\to 1} n(x) = 1.54$ (x is the zirconia weight fraction) compared to 1.79 in our zirconia film. This can be attributed to lower porosity in our materials as indicated also by the relative high density. As expected,[1] the films become thicker as the GLYMO content increases.

It is noteworthy that the deviations of both densities and refractive indices measured from the calculated values become greater as the zirconia content increases. This phenomenon was attributed to the increasing porosity of the films. Close examination of Wang and Wilkes's[19] results reveals a similar pattern—very slow increase (if any) in refractive index as the Zr content increases between 30 and 60%. We did not calculate the volume fraction of the pores from this deviations because it is difficult to determine the exact content of absorbants in the thin film pores and their contribution to the refractive index. Generally, the refractive index is a little higher than in titania-containing films[1] (~1.75) and it is sufficient to obtain multimode waveguides on soda lime glass support.

(17) Jansen, M.; Guenther, E. *Chem. Mater.* **1995**, *7*, 2110.
(18) Doeuff, S.; Dromzee, Y.; Taulelle, F.; Sanchez, C. *Inorg. Chem.* **1989**, *28*, 4439.
(19) Wang, B.; Wilkes, G. L. *J. Polym. Sci., A* **1991**, *29*, 905.

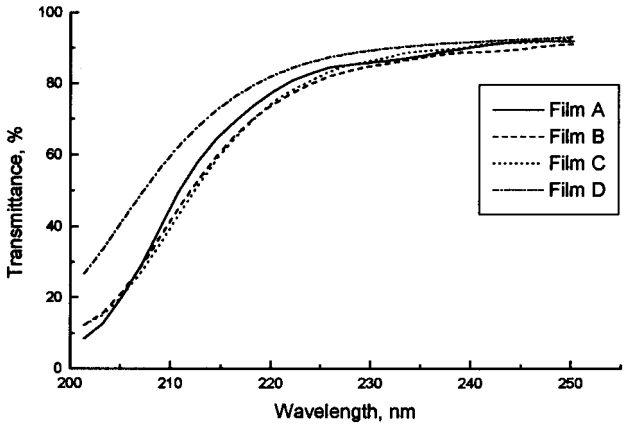

Figure 2. Transmission spectra of zirconia and zirconia−GLYMO films (curves labels according to Table 1).

The transmittance spectra of the films deposited on the optical quartz plates are shown in Figure 2. In zirconia (film A) case the film is transparent from ∼220 nm. Introduction of GLYMO has no significant effect. Only at high GLYMO content (70%, film D) does the film become more transparent, probably due to the lower porosity (lower scattering) or decrease of size of ZrO_2 clusters that increases in the energy gap between the valence and conduction bands due to quantum localization of the electron and the hole.

FTIR Spectra. The spectrum of the films made from zirconium propoxide (Figure 3a) with no ORMOSIL is identical to that of the precipitate formed in the solution before the addition of water or propanol to the $Zr(OPr^n)_4$ and acetic acid mixture. The bands at 475 and 650 cm^{-1} are the Zr−O−Zr and Zr−O vibrations, respectively.[20] The broad band at 1027 cm^{-1} is attributed to the presence of propoxy groups (ν(C−O)).[20] The bands at 1445 and 1555 cm^{-1} are the symmetric and antisymmetric stretching frequencies, respectively, of the acetate groups, and it is difficult to determine from the spectrum whether the acetate acts as a chelating or bridging ligand. The energy difference between the two bands $\Delta = 110$ cm^{-1}. According to Doeuff et al.[21] the energy separation in bridging acetate usually lies between 120 and 160 cm^{-1} and lower Δ values indicate chelating bonding. Laaziz et al.,[20] on the other hand, have identified the band at 1557 cm^{-1} as the antisymmetric stretching of acetate group attached to Zr ions (their assignment was also verified by a single-crystal X-ray analysis).

The spectra of the Zr−GLYMO films is shown in Figure 3 (b, film C; c, film D). The Zr−O−Zr bond remains in those spectra even at high GLYMO to zirconia ratio. This indicates that the homocondensation reaction that forms the Zr−O−Zr bonds is favored on the heterocondensation reaction that forms the Zr−O−Si bonds. As the GLYMO content increases this bands appears at lower energies: from 476 cm^{-1} in films prepared without GLYMO to 472 cm^{-1} in films containing 57 mol % GLYMO and to 466 cm^{-1} in a film containing 69 mol % GLYMO. Even though this shift is small it is consistent with Jansen et al.'s[17] results: 476 cm^{-1} in zirconia and 468 cm^{-1} in zircon.

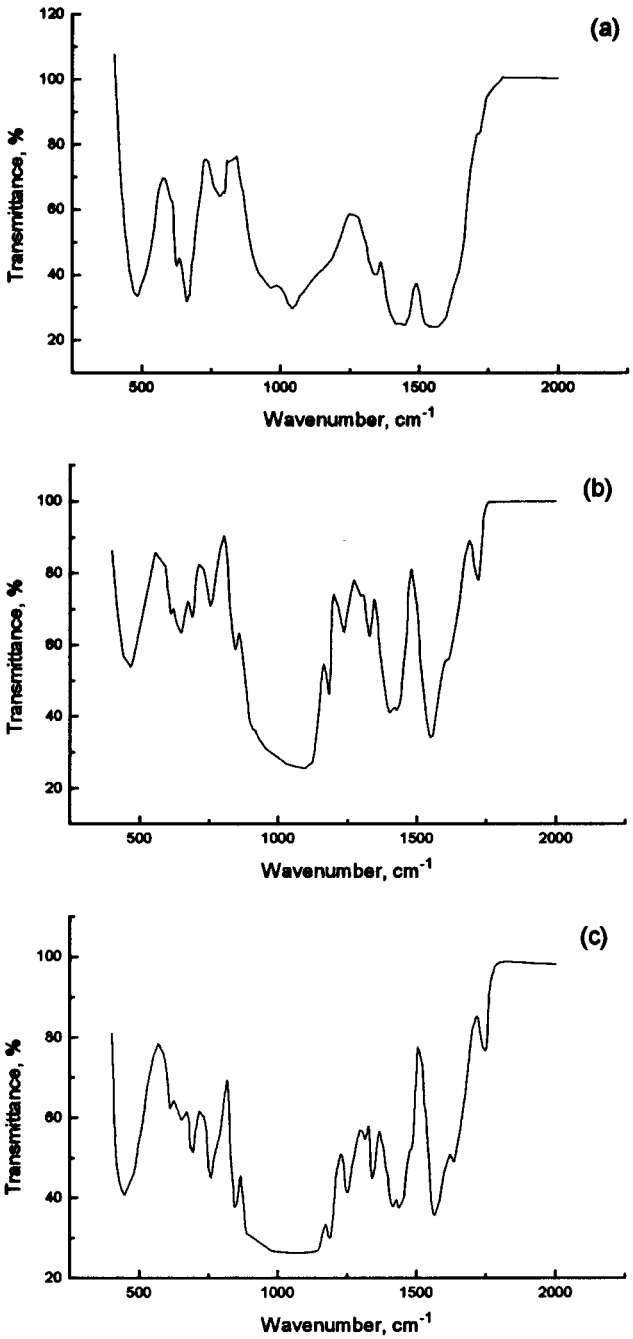

Figure 3. FTIR spectra (a) of film A (zirconia) and (b and c) films C and D (zirconia−GLYMO), respectively.

The presence of homocondensation products can be attributed to the higher rate of hydrolysis of zirconium alkoxides (even chelated) compared to that of silicon alkoxides[22] and/or to oligomeric structure of the Zr precursor (see Discussion).

An absorption band appears at ∼850 cm^{-1} that is attributed to Zr−O−Si bonds by Jansen et al.[17] As the GLYMO content increases, this band becomes stronger. Some publications[23] assigned the band at ∼1020 cm^{-1} to this bond, but our results show that this absorption band is found also in films prepared with no silane at all. We, therefore, followed Laaziz et al.[20] in attributing this band to the C−O stretching vibration in the propoxy

(20) Laaziz, I.; Labort, A.; Julbe, A.; Guizard, C.; Cot, L. *J. Solid State Chem.* **1992**, *98*, 393.
(21) Doeuff, S.; Henry, M.; Sanchez, C.; Livage, J. *J. Non-Cryst. Solids* **1987**, *89*, 206.
(22) Brinker, C. J.; Scherer, G. W. *Sol-gel Science*; Academic Press: New York, 1990.
(23) Wellbrook, U.; Beier, W.; Frischat, G. H. *J. Non-Cryst. Solids* **1992**, *147* and *148*, 350.

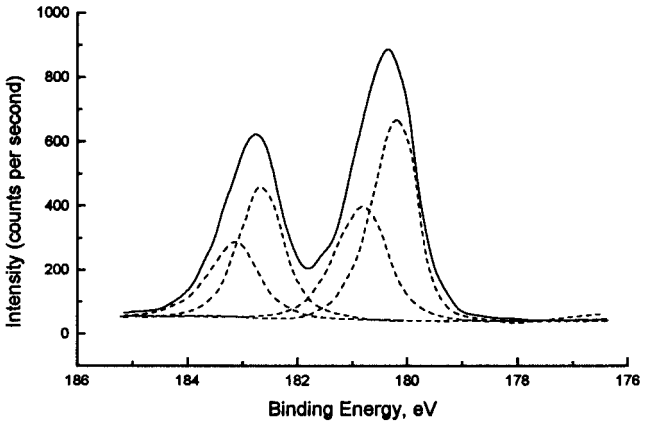

Figure 4. Zr 3d line in the XPS spectra of zirconia film (film A).

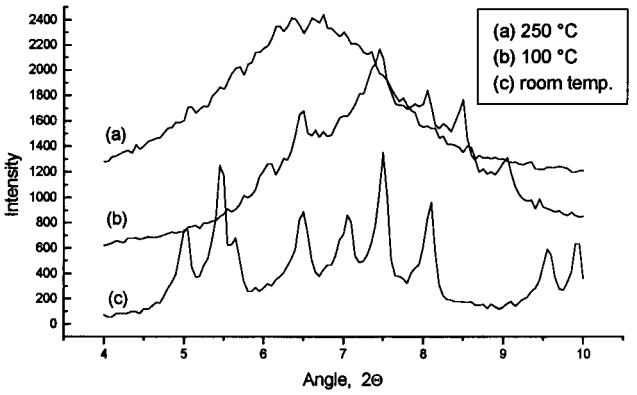

Figure 5. XRD patterns of precipitate (a) at 250 °C, (b) heated to 100 °C, and (c) at room temperature.

group. The acetate bands in the Zr−GLYMO spectra are characteristic of bridging bidentate acetate $\Delta = 155$ cm^{-1}. Additional band appears at 1735 cm^{-1} indicating the presence of monodentate acetate[21] attached to the silicon atom as was also noted in Ti−GLYMO films.[2] At ~1100 cm^{-1} typical silica bands are observed; this demonstrates (like the Zr−O−Zr strong bands) the homocondensation reaction occurring between the GLYMO molecules.

XPS Measurements. *Zirconia Films.* The Zr 3d binding energy spectrum showed asymmetry as shown in Figure 4. This line shape can be convoluted using two doublets, one at 182.2 eV (fwhm = 0.97) and one at 182.9 eV (fwhm = 1.05). The split is quite small (0.7 eV) if compared to the fwhm (0.97 eV), but large enough to produce significant asymmetry. We attributed the high binding energy component to zirconium ions bonded to oxygen while the lower binding energy component is attributed to Zr ions bonded to organic ligands which are less electronegative—acetate and propoxide. Similar splitting was observed in titania films prepared by similar procedure.[2] In our case, however, the fraction of ions attached to organic ligands is much higher, about 40% compared to about 20% in the titania films.[2]

The C 1s spectrum consist of three peaks: one at 284.6 eV attributed to alkyl carbon, a peak at 286.2 eV attributed to alkoxy groups, and a peak at 288.8 eV attributed to carboxyl carbon atoms. The atomic percentage of the alkyl, alkoxy, and carboxylic carbons are 23, 4, and 13, respectively. Since every acetate group donates one alkyl and a propoxy group donates two alkyl carbons, the expected percentage of alkyl carbons is 21, fairly close to the measured 23%. The O 1s spectrum consists of two components at 529.6 and 531.6 eV attributed to backbone (oxides) and ligand (acetate, propoxy, and hydroxyl groups), respectively; the ratio of backbone oxygen to ligand oxygen is 0.31.

The ratios found between the atomic percentages of the different components are carboxylic carbons/zirconium = 1.0; alkoxy carbons/zirconium = 0.3; and backbone (oxide) oxygen/zirconium = 0.9. This finding suggests the existence of a third type of ligand attached to the zirconium ions. The composition: $ZrO_{0.9}(OAc)$-$(OPr)_{0.3}(OH)_{0.9}$ explains the amount of ligand oxygen (expected ratio between backbone and ligand oxygen: 0.28) and the "deficiency" in organic ligands. The mass percentage for this composition is H 3.1%, C 17.7%, O 33.4%, and Zr 45.8%. The carbon content of the precipitate found from combustion was 19.15%. The decrease can be attributed to further hydrolysis upon water addition to the precipitate.

Zirconia−GLYMO Films. Two significant features were observed in the XPS measurement of Zr-GLYMO films.

1. The oxide oxygen to Zr ratio remains the same as in the zirconia films; a decrease in the carboxylic oxygen to Zr ratio is observed from 1:1 in zirconia film to 1:5 in the Zr−GLYMO film (film B according to Table 1) and this finding can be attributed to replacement of the acetate by Zr−O−Si bond. The preservation of the oxide fraction is in agreement with the appearance of typical Zr−O−Zr absorption bands in the FTIR spectra. We did not observe significant changes in those features, depending on the Si content of the films.

2. There were major changes in the composition of the surface as compared to the film depth composition measured when the surface of the film was removed by ion sputtering of about 1−2 nm. The zirconium content in the surface is 30−40% of the zirconium content in the film depth. The silicon content on the surface is about half the content in the film depth. The surface layer is very rich in carbon (in view of surface energy consideration), and the alkyl carbon content of the surface remains as in the depth (or even slightly lower then in the depth) but the concentration of carbon having binding energy for C 1s of 286 eV, i.e., amounts of C−OH and C−O−C groups, is 3 times higher on the surface than in the bulk. This finding indicates that the surface is composed mainly of the organic residues of the GLYMO and, maybe, solvent's residues bonded to it. It should be noted that preferential sputtering of low mass ions[24,25] should be taken in account, but it cannot be fully responsible for such large and characteristic changes.

XRD Patterns of Precipitate and Films. *Precipitate.* XRD patterns of precipitate (intermediate) show (Figure 5) unidentified wide peaks at angles in area of 4−10°. These peaks can be accorded to oligomeric structures with *d* spacing values of about 10 Å. Similar values were identified in a titanium oxoacetates precipitates[26] and hexanuclear titanium alkoxyacetate

(24) Mukhopadhyay, S. M.; Garofalini, S. H. *J. Non-Cryst. Solids* **1990**, *126*, 202.
(25) Czanderna, A. W., Ed. *Methods of surface analysis*; Elsevier Scientific Publishing Co.: Amsterdam, 1975.
(26) Doeuff, S.; Henry, M.; Sanchez, C. *Mater. Res. Bull.* **1990**, *25*, 1519.

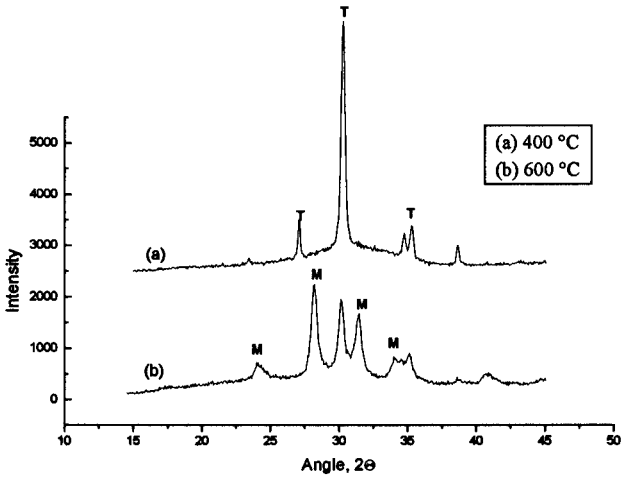

Figure 6. XRD patterns of precipitate heated to 400 °C (a) and 600 °C (b).

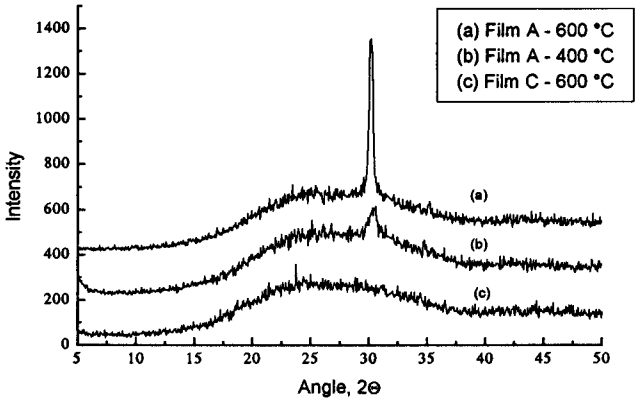

Figure 7. XRD patterns of film A heated to 600 °C (a) and 400 °C (b) and film C heated to 600 °C.

complex.[27] Such trimer condensation products are intermediate in the network formation and it is reasonable to assume similar species in the early stages of condensation in our system. It should be noted that no peaks of zirconium acetate were found. Upon heating of the precipitate at 250 °C, clear signs of amorphization are seen. This fact can be attributed to partial elimination of chelating organic ligands (see data of thermal analysis below). The heating up to 400 °C (Figure 6) promotes total disappearance of peaks at small angles and only peaks of tetragonal form of ZrO_2 are found. With the heating up to 600 °C appears also monoclinic form of zirconium dioxide.

Films. XRD of films show a big similarity with the XRD of the precipitate, with broad bands at the same angles; however films, without thermal treatment, remain amorphous.

Film A (only zirconia based) after heating at 400 and 600 °C shows (Figure 7) peaks of tetragonal form of ZrO_2 only (more intensive peaks at 600 °C). Film C even after such heating remains amorphous. XRD of both heated films show disappearance of peaks at small angles.

These results are similar to results of Jansen et al.[17] and Ward et al.[28] The differences between patterns of film A and precipitate heated to 600 °C can be explained by the presence of cross-linked network in the case of

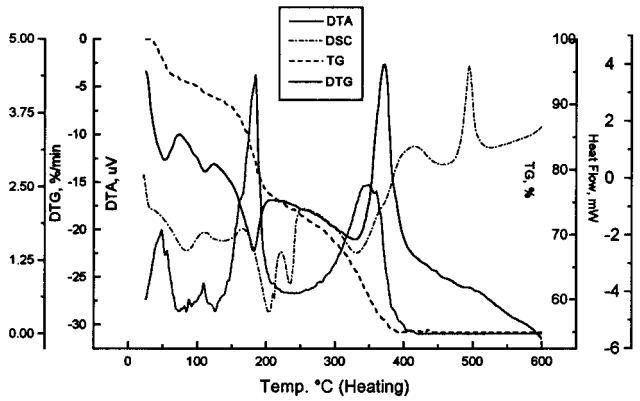

Figure 8. DTA/TG/DTG (air atmosphere, reference Al_2O_3) and DSC (argon atmosphere) of precipitate (heating rate 10 °C/min).

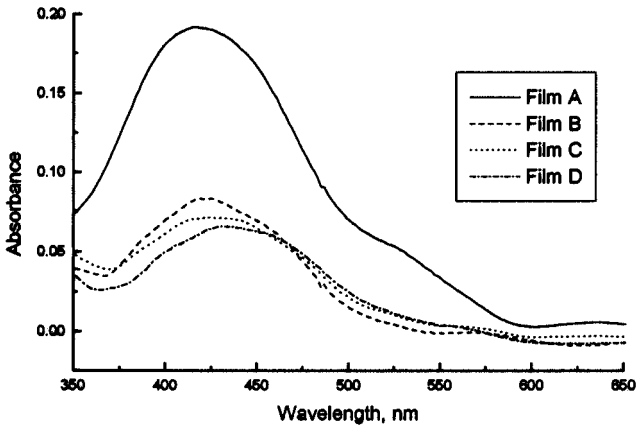

Figure 9. Absorption spectra of Methyl Red in zirconia and zirconia−GLYMO films (curves labels according to Table 1).

film and the more open structure of precipitate, which through thermal destruction produces more nuclei of crystallites. This, according to Ward et al.,[28] facilitates crystallization of monoclinic form at the lower temperatures.

Thermal Analysis. On the DTA/TG/DTG curves and on the DSC curve (Figure 8) of the precipitate we can see the peaks of evaporation of the solvents (70−130 °C), peaks of thermal destruction of zirconium propoxyacetate (170−240 °C), formation of tetragonal form of zirconia (320−330 °C), and tetragonal to monoclinic phase transition at 490 °C. These results are in full agreement with the data of X-ray diffraction and the results of Ward et al.[28]

The differences in peak positions between the DTA/TG and DSC curves (mainly at lower temperatures) are well-known[29] and can be explained by differences in methods and in the experiment conditions.

Absorption Spectra of Methyl Red (MR) in the Films. In the spectrum of MR in zirconia film (Figure 9, curve A) appears mainly basic (anionic)[30] form of MR having absorption peak at 415 nm. This finding can be accorded to the presence of acetate groups, which are Lewis bases, and their presence in the final product is proven by FTIR and XPS. In zirzonia−GLYMO films (Figure 9, curves B, C, D) a shoulder appears at about 460 nm, attributed to the neutral form of the dye.

(27) Gautier-Luneau, I.; Mosset, A.; Galy, J. *Z. Kristallogr.* **1987**, *180*, 83.
(28) Ward, D. A.; Ko, E. I. *Chem. Mater.* **1993**, *5*, 956.
(29) Wendlandt, W. W. *Thermal methods of Analysis*; J. Wiley & Sons: New York, 1974.
(30) Livingston, R.; Parisser, R. *J. Am. Chem. Soc.* **1948**, *70*, 1510.

Yariv[31] showed that in pure GLYMO glass, the dye is presented in its acidic form. The presence of the neutral form indicates that the dye is influenced by the average environment of the "basic" zirconia and the "acidic" GLYMO.

Films were exposed to vapors of hydrochloric acid and ammonia in desiccators and showed fast response times (about 3 s) and full reversibility.

Discussion

It should be noted that the zirconium propoxide precursor forms trimeric units in which the Zr ion is in octahedral coordination.[32] Recently XAFS measurement made by Helmerich[33] supported that proposed structure. Those units are the "building blocks" in the formation of the Zr oxide−alkoxide polymers, which are the intermediate products in the synthesis of alkoxide-derived zirconia-based materials.[34] In particular, in water concentrations $H_2O/Zr > 1$, $Zr(OPr^n)_4$ acts according to model III proposed by Bradley et al.[35] for Ti oxide−alkoxide intermediates; *i.e.*, after partially hydrolysis forms $Zr_2O_3(OPr)_2(PrOH)_4$ or $Zr_3O_6(PrOH)_6$, the highest polymer possible according to this model is the trimer (unlike model I,[35] which enables the formation of infinite polymer) and a large oxide network is formed only upon evaporation of the solvent. The carboxylic acid replaces a terminal alkoxide with chelating carboxylate[33] and does not change the oligomeric structure.[36]

Products of the chelation and partial hydrolysis and condensation of zirconium and titanium alkoxides were isolated as single crystals by Gautier-Luneau et al.,[27] Laaziz et al.,[20] and S. Doeuff et al.[18] The titanium ethoxide derived product prepared by Gautier-Luneau[27] was a hexanuclear titanium acetate complex and is built up of two trinuclear oxo-centered units. The titanium zirconium product of the two *n*-propoxide by Laaziz[20] was $Zr_6Ti_3(OPr)_{16}(OAc)_8O_6$ (two trimers of zirconium and one trimer of titanium). It can be generalized that the metal's trimers are the fundamental units that combined to form the oxide. Our results are in agreement with this model:

1. The FTIR spectra shows the presence of homonucleation products: Zr−O−Zr and Si−O−Si bonds. This finding can be explained by the oligomeric structure since only the terminal ligands can participate in an hydrolysis and heterocondensation reaction to give a Zr−O−Si bond. However, the mixed oxide was present in higher proportion than in a hybrid titania−GLYMO, because of the tendency of the titanium alkoxide precursors to form infinite oxide−alkoxide chains (model I according to Bradley et al.[35]) in contrast to the stable trimer of the zirconium oxide−alkoxide present in our system.

2. The XPS measurements showed the presence of two zirconium ion populations, one that is attributed to zirconium bonded to backbone oxygen nd one at lower binding energy that can be attributed to terminal zirconium ions in the clusters. In the composite films the oxide fraction remains unchanged and the acetate content decreases which indicates that Zr−O−Si bonds are formed by condensation of the oligomers and leaving of the terminal acetate ligand.

3. The oligomeric nature of the precipitate and the zirconia present in the final product is shown in the X-ray diffraction results (Figure 4).

4. The spectra of the MR molecules embedded in the film show the presence of one dye population. In contrast, the spectrum of MR embedded in hybrid titania−GLYMO films[2] shows the presence of two dye populations that are not in equilibrium—one in the titania phase and one in the ORMOSIL phase. This difference can be explained by the higher homogeneity of the Zr−GLYMO glass compared with the Ti−GLYMO glass.

As noted above, refractive indices of the films are sufficient to obtain waveguiding on glass support. The potential problem in real applications can be a scattering and, therefore, losses, promoted by nanostructures, such as oligomeric fragments of the matrix. Losses also can be promoted by the other factors, so further detailed study of the attenuation is planned; however, scattering was not found to be a severe prlblem in other waveguiding systems with the similar nanoparticle sizes (titania−ORMOSIL films[2]).

It should be noted that we found no solubility of the films in water and all the films, even based on zirconia only, are hydrophobic. This finding shows that zirconia-based films can be used in chemical sensors also for water media.

Conclusions

In this work we describe for the first time zirconia-based planar waveguides, synthesized at room temperature. This procedure opens new opportunities for optical and analytical applications. Zirconia-based waveguides seem to be suitable chemically inert matrixes for immobilization of laser dyes, reagents with high nonlinear susceptibility, and analytical reagents.

The combination of high porosity, chemical resistance, and waveguiding can be applied for building simple, one-layer sensors for environmental impurities. The first attempt to such sensors was shown in this work on example of Methyl Red.

Acknowledgment. We are grateful to Dr. I. Lapides for fruitful discussions, to Dr. H. Cohen, Dr. A. Givan, Dr. D. Golodnizki, and A. R. McGhie for their help, to U. Wolf for kindly allowing us to use his equipment, and to E. Faraggi for his catalytic activity. We are also grateful to Austrian Bank providing the fellowship to M.Z.

CM960135X

(31) Yariv, E. M. Sci. Thesis, submitted to the Hebrew University, Jerusalem, Israel, 1992.
(32) Bradley, D. C.; Mehrotra, R. C.; Swasnwick, J. D.; Wardlaw, W. *J. Chem. Soc.* **1953**, 2025.
(33) Helmerich, A.; Raether, F.; Peter, D.; Bertagnolli, H. *J. Mater. Sci.* **1994**, *29*, 1388.
(34) Bradley, D. C.; Carter, D. G. *Can. J. Chem.* **1961**, *39*, 1434.
(35) Bradley, D. C.; Gaze, R.; Wardlaw, W. *J. Chem. Soc.* **1957**, 469.
(36) Peter, D.; Ertel, T. S.; Bertagnolli, H. *J. Sol-Gel Sci. Technol.* **1995**, *5*, 5.